NUCL SCI TECH (2017) 28:18
DOI 10.1007/s41365-016-0175-6

Production of neutron-rich exotic nuclei in projectile fragmentation at Fermi energies

R. Ogul[1] · N. Buyukcizmeci[1] · A. Ergun[1] · A. S. Botvina[2,3]

Received: 28 April 2016 / Revised: 20 June 2016 / Accepted: 1 July 2016 / Published online: 24 December 2016

Abstract Isotopic fragment yields of projectile fragmentation in peripheral collisions of ^{86}Kr on ^{124,112}Sn and the mean neutron-to-proton ratios of the fragments are calculated, theoretically, within the ensemble approach of statistical multifragmentation model. Obtained data are compared to the experimental cross-section measurements for the projectile-like fragmentation in the reaction of 25 MeV/nucleon ^{86}Kr+^{124,112}Sn at Texas A&M University. We show the enhancement in the production of neutron-rich isotopes close to the projectile as observed in the experiments. We also demonstrate the universality of the limitation of the excitation energy induced in the projectile residues.

Keywords Projectile fragmentation · Peripheral collisions · Isotope productions · Universality

1 Introduction

One of the most interesting studies of nuclei far from stability is the production of exotic nuclei in various reactions over a wide range of energy. These reactions are mainly consisting of fission, fusion, nuclear fragmentation, and nucleon transfer. At high energies, above the Fermi energy regime, exotic beams over the entire periodic table, up to uranium, are produced by nuclear fragmentation of relativistic projectiles [1–3]. At low energies near the Coulomb barrier (1–10 MeV/nucleon), neutron-deficient isotopes are produced as a result of the fusion of heavy ions in central collisions. This is because the increase in neutron excess for the heavier nuclei leads to the formation of proton-rich exotic nuclei close to the proton dripline. Similarly, heavier neutron-rich, as well as neutron-deficient, isotopes are produced as a result of multinucleon transfer reactions (consecutive proton captures) through the rp-process, the so-called nucleosynthesis. At energies over the Coulomb barrier, up to the Fermi regime, however, neutron-rich isotopes are populated in deep inelastic transfer (DIT) reactions [4–6]. Starting from the Fermi energies, nuclear multifragmentation reactions become superior to other reaction channels [7–11], and one may possibly study the neutron-rich isotope production from projectile fragmentation in Fermi energy regime (20–40 MeV/nucleon). There exist numerous models in the literature to calculate the production cross sections of exotic nuclei for interpretation of experimental data for various reaction channels. These models generally consider a simulation of the formation of an intermediate nucleus as a first step, and then a de-excitation process is treated with an evaporation code [12, 13]. In this study, we shall consider the ensemble version of the statistical multifragmentation model for the interpretation of data given in Ref. [7]. In the ensemble approach, formation of the equilibrated nuclear system is defined by a dynamical approach, and formation of hot fragments and de-excitation processes are defined by statistical multifragmentation model.

✉ N. Buyukcizmeci
nihal@selcuk.edu.tr

[1] Department of Physics, University of Selçuk, 42079 Konya, Turkey

[2] ITP and Frankfurt Institute for Advanced Studies, J.W. Goethe University, 60438 Frankfurt am Main, Germany

[3] Institute for Nuclear Research, Russian Academy of Sciences, Moscow, Russia 117312

In this work, our theoretical analysis is based on the experimental cross-section measurements for the projectile-like fragmentation from the reactions of 25 MeV/nucleon ^{86}Kr+^{124,112}Sn at Texas A&M University given in Ref.[7]. In the present calculations, we used the ensemble approach [14] based on the statistical multifragmentation model (SMM) [15], which was also used for the analyses of the experimental data of FRS (fragment separator) measurements [16] at GSI laboratory at the relativistic beam energies of 1 GeV/nucleon for the fragmentation of ^{124,112}Sn and ALADIN data at 600 MeV/nucleon for ^{124}Sn, ^{107}Sn, and ^{124}La projectiles [17]. We also used a single-source simulation of SMM within the markov chain process for the analyses of MSU and FAZIA experimental data measured at the beam energy of 50 and 35 MeV/nucleon for the reactions of ^{124,112}Sn+^{124,112}Sn and ^{84}Kr+^{112,124}Sn, respectively. The obtained results were in close agreement with the data [18–20].

2 Statistical approach to multifragmentation

In the statistical ensemble approach, the multifragmentation process is subdivided into (a) a dynamical stage leading to the formation of an equilibrated nuclear system, (b) the disassembly of the system into individual primary fragments, and (c) the subsequent de-excitation of the hot primary fragments. In the dynamical stage, the formation of the ensembles of excited residual nuclei is determined with the intranuclear cascade (INC) model [21]. Fragmentation of the system and the de-exitation process are described by SMM as including all breakup channels composed of nucleons and excited fragments, and during each partitions the laws of conservation of energy, E^*, momentum, angular momentum, mass number, A, and charge number, Z, are considered. Besides the breakup channels, the compound-nucleus channels at low excitations are also included, and competition between all channels is permitted. In this way, the SMM covers the conventional evaporation and fission processes occurring at low excitation energy as well as the transition region between the low- and high-energy de-excitation regimes. In the thermodynamic limit, SMM is consistent with liquid–gas phase transition when the liquid phase is represented by infinite nuclear cluster. In the microcanonical treatment, the statistical weight of a breakup channel is calculated as an exponential of the entropy of the system in this channel as follows:

$$W_j \approx \exp(S_j(E^*, A, Z)), \tag{1}$$

where S_j is the entropy of the system in channel j. The decay channels (partitions) are generated uniformly in the phase space by the Monte Carlo method according to their statistical weights. Light fragments, with mass number $A \leq 4$ and charge number $Z \leq 2$, are considered as elementary particles with the corresponding spins (nuclear gas) that have a translational degree of freedom. The fragments with mass number $A > 4$ are treated as heated nuclear liquid drops. In this way, one can study the nuclear liquid–gas coexistence in the freeze-out volume. Free energies, $F_{A,Z}$, of each fragment are parameterized as a sum of the bulk, surface, Coulomb, and symmetry energy contributions as follows:

$$F_{A,Z} = F^B_{A,Z} + F^S_{A,Z} + E^C_{A,Z} + E^{\mathrm{sym}}_{A,Z}. \tag{2}$$

The bulk contribution is given by $F^B_{A,Z} = (-W_0 - T^2/\varepsilon_0)A$, where T is the temperature, the parameter, ε_0, is related to the level density, and $W_0 = 16$ MeV is the binding energy of infinite nuclear matter. Contribution of the surface energy is $F^S_{A,Z} = B_0 A^{2/3}[(T_c^2 - T^2)/(T_c^2 + T^2)]^{5/4}$, where $B_0 = 18$ MeV is the surface energy term and $T_c = 18$ MeV is the critical temperature of the infinite nuclear matter. Coulomb energy contribution is $E^C_{A,Z} = cZ^2/A^{1/3}$, where c denotes the Coulomb parameter obtained in the Wigner–Seitz approximation, and $c = (3/5)(e^2/r_0)(1 - (\rho/\rho_0)^{1/3})$, with the charge unit, e, $r_0 = 1.17$ fm, and ρ_0 is the normal nuclear matter density (0.15 fm^{-3}). And finally, the symmetry term is $E^{\mathrm{sym}}_{A,Z} = \gamma(A - 2Z)^2/A$, where $\gamma = 25$ MeV is the symmetry energy parameter. All the parameters given above are taken from the Bethe–Weizsäcker formula and correspond to the assumption of isolated fragments with normal density unless their modifications in the hot and dense freeze-out configuration follow the analysis of experimental data. The freeze-out density of one-third of the normal nuclear matter density is assumed in our previous studies and is consistent with independent experimental determination in sources formed in peripheral nuclear collisions. In this work, the freeze-out density is taken to be $\rho = (1/6)\rho_0$, which takes into account the additional expansion as a result of the flow development. In the present calculations, we follow the procedure used by Botvina et al. [22] and apply the same approach used in Ref. [17]. At low excitation energies ($E^* < 1$ MeV/nucleon), the SMM code can also be used to describe the de-excitation process of primary hot fragments on the basis of standard Weisskopf evaporation and fission scheme (see, e.g., Ref. [15]).

3 Charge and isotopic distributions

Charge distributions predicted by the SMM ensemble calculations for the fragments of the quasiprojectiles ^{86}Kr, ^{90}Kr, and ^{92}Kr with different neutron-to-proton ratios are

shown in Fig. 1 as a function of the atomic number, Z, of the final fragments. In this work, we assume that neutron rich ^{92}Kr and ^{90}Kr quasiprojectiles are formed in deep inelastic transfer as a result of the interactions between projectile and target nuclei in the two studied reactions ^{86}Kr+^{124}Sn and ^{86}Kr+^{112}Sn, respectively, at 25 MeV/nucleon. Choosing the quasiprojectiles as ^{92}Kr and ^{90}Kr provided us with optimum agreement between our predictions and experimental data given in Ref. [7]. According to DIT, at the first stage of the collisions, the multineutron pickup (up to 6–8 neutrons) procedure can be described reasonably well to produce quasiprojectiles. This shows the importance of the neutron richness of the target in the production mechanism. The excitation energy induced may be below the particle evaporation threshold at low energies. In this case, the SMM also covers the de-excitation process of primary hot fragments through the Weisskopf evaporation. The theoretical results for charge distributions of the final fragments shown in Fig. 1 were obtained from ensemble calculations performed for 500,000 reaction events with the standard SMM ensemble parameters used in the analysis of the ALADIN data in Ref. [17]. Even if this ensemble of sources was verified for residues formed in peripheral relativistic collisions, we believe that it can be applied as a qualitative estimate for peripheral heavy-ion collisions at the Fermi energy too since the universality of the limitation of the excitation energy residing in the ensemble of the equilibrized projectile residues may exist in the both cases. The predicted distributions for neutron-poor and neutron-rich elements are very similar for the lighter fragments but qualitatively different for the heavier fragments close to the projectile, which are not produced in multifragmentation.

The mean neutron-to-proton ratios, N/Z, of the final fragments are important for the interpretation of isotope production when it is related to the equation of the state of asymmetric nuclear matter through the symmetry term. In Fig. 2, we show the variation of N/Z with charge number up to $Z = 36$. It is shown in this figure that N/Z ratios for the neutron-poor element, ^{86}Kr, are lower than those of the neutron-rich elements, ^{90}Kr and ^{92}Kr. In other words, neutron-rich systems preferentially populate the most neutron-rich isotopes (with higher N/Z values), and the memory of the N/Z of the initial projectile system is seen to be preserved for all isotope distributions. This is in agreement with our previous interpretation of experimental analyses [16, 17].

In high- and intermediate-energy projectile fragmentation reactions, the target has almost no effect on the production cross section of neutron-rich nuclides. In contrary, at low energies above the Coulomb barrier, the neutron-to-proton ratio of the target has a strong influence on the production of neutron-rich isotopes in multinucleon transfer reactions. In this case, neutron pickup and proton-

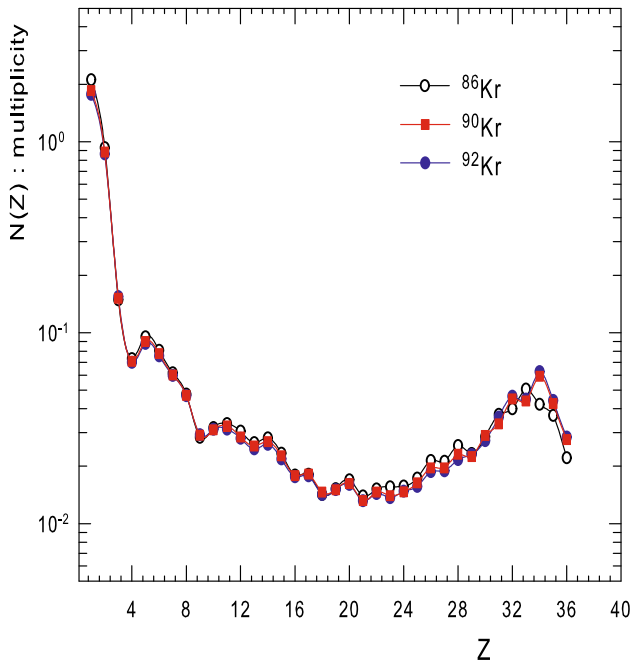

Fig. 1 (Color online) Charge distributions of fragment products from ^{86}Kr (*empty circles*), ^{90}Kr (*full squares*), and ^{92}Kr quasiprojectiles (*full circles*) as obtained from ensemble calculations with standard parameters. Here, ^{92}Kr and ^{90}Kr quasiprojectiles are formed in ^{86}Kr+^{124}Sn and ^{86}Kr+^{112}Sn reactions, respectively, and ^{86}Kr is assumed to be formed in any reaction without neutron transfer

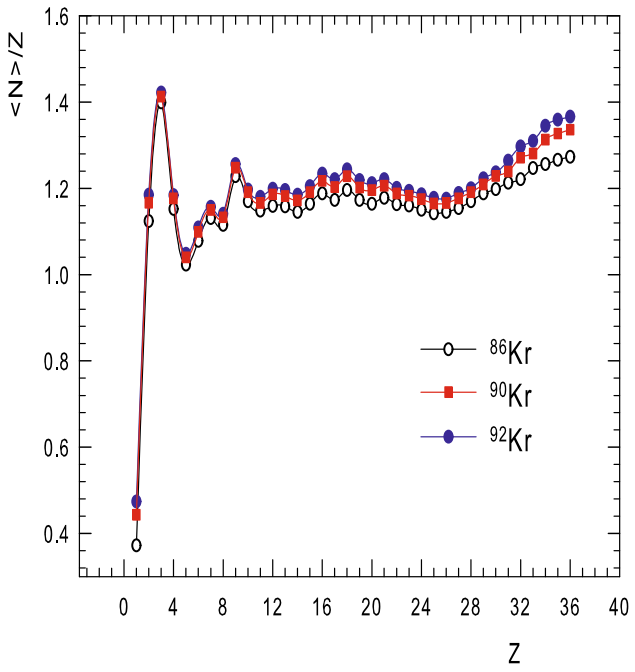

Fig. 2 (Color online) Mean N/Z values of fragment products from ^{86}Kr (*empty circles*), ^{90}Kr (*full squares*), and ^{92}Kr (*full circles*) quasiprojectiles. Notations are as in Fig. 1

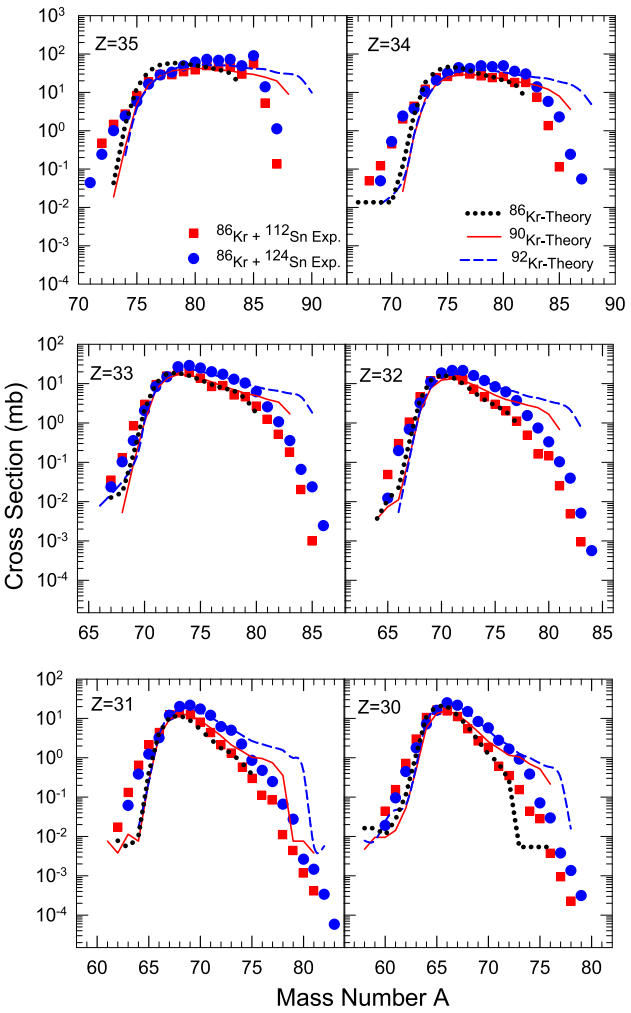

Fig. 3 (Color online) Isotope mass distributions (cross sections) of projectile fragmentation of ^{86}Kr (*dotted lines*), ^{90}Kr (*solid lines*), and ^{92}Kr (*dashed lines*) and corresponding experimental data for ^{86}Kr+^{124}Sn (*full circles*) and for ^{86}Kr+^{112}Sn (*full squares*) reactions at 25 MeV/nucleon projectile energies as defined in Fig. 1

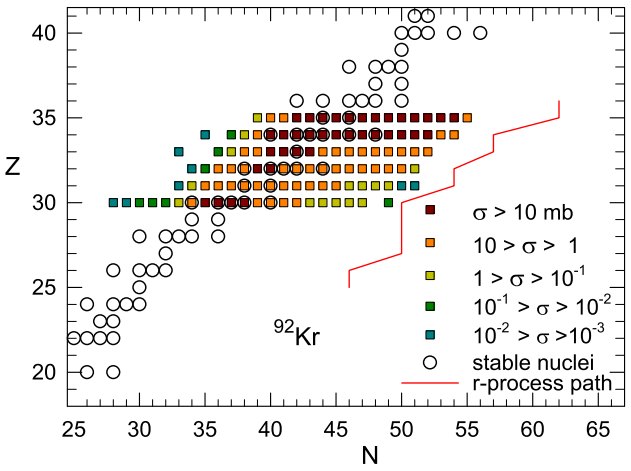

Fig. 4 (Color online) Production cross sections of the fragments $Z = 35 - 30$ from quasiprojectile, ^{92}Kr, as predicted by SMM ensemble calculations and their location with respect to the *r*-process path (*solid line*)

stripping channels are dominant for the production of neutron-rich nuclides. At Fermi energies, nucleon exchange models are developed to describe the first stage of the formation of hot projectiles. In our simulations, we consider six and four neutrons picked up by the projectile ^{86}Kr in the reactions ^{86}Kr+^{124}Sn and ^{86}Kr+^{112}Sn, respectively, for the production of more neutron-rich quasiprojectiles, ^{92}Kr and ^{90}Kr.

In Fig. 3, we show the mass distributions for near-projectile elements, $Z = 35 - 30$, from the two studied reactions, ^{86}Kr+^{124}Sn and ^{86}Kr+^{112}Sn at 25 MeV/nucleon, as a function of the mass number, A, of the final fragments. The experimental results (full circles and squares) are taken from Ref. [7]. The dashed and solid lines show the theoretical results obtained from ensemble calculations for the quasiprojectiles ^{92}Kr and ^{90}Kr, respectively, performed for 500,000 reaction events with the standard SMM parameters. To permit a more quantitative comparison of the model results with the experimental data, the SMM ensemble calculations were normalized with respect to the measured elemental cross sections. The obtained factors are 0.0078, 0.0057, 0.0054, 0.0079, 0.0124, and 0.0255 mb per theoretical event for $Z = 30, 31, 32, 33, 34$, and 35 from ^{92}Kr quasiprojectile, respectively, and similarly for ^{90}Kr and ^{86}Kr. First, we studied ^{86}Kr quasiprojectile fragmentation, and it was seen that the yields of neutron-rich isotopes close to the projectile mass number were insufficient to cover the experimental data. In Fig. 3, we show that the predicted results for ^{92}Kr and ^{90}Kr quasiprojectile fragmentations reproduce the experimentally observed isotope yields in the reactions ^{86}Kr+^{124}Sn and ^{86}Kr+^{112}Sn, respectively. One may observe that the neutron-rich fragment yields produced in the reactions with the more neutron-rich ^{124}Sn target are considerably larger than those obtained in the reactions with the less neutron rich ^{112}Sn for both theoretical and experimental results. This supports the idea of nucleon exchange at the first stage and the important role of the target in the neutron-rich isotope production in peripheral collisions near Fermi energy. The observed agreement between the experimental and theoretical results is satisfactory enough, qualitatively, and considerable differences exist in the yields. In the neutron-rich side of the isotopic curve in Fig. 3, one may see that theoretically predicted yields are at least some orders of magnitude larger, with respect to the measured yields, for both reactions. The main reason for this difference may stem from the fact that the isotope distributions were not always fully covered in the experiment, thus causing the observed differences in the yields. Therefore, one should take the experimental filter into account for a

more detailed comparison with experimental data. The results for the location of neutron-rich and proton-rich fragments in the chart of the nuclides are illustrated in Fig. 4, with respect to the astrophysical *r*-process path. The production cross sections of the final exotic nuclides are shown by full squares with colors classified according to the values of the cross sections, while the stable nuclei are shown with empty circles in each production channel. It is seen from this figure that very neutron-rich nuclei toward the neutron dripline can be produced within peripheral heavy-ion collisions by radioactive neutron-rich beams.

4 Conclusion

We show that our theoretical results reproduce the experimentally observed enhancement in the neutron-rich isotope production by using the neutron-rich targets at low energies near the Fermi energy regime. This enhancement is associated with peripheral interactions of the neutron-rich ^{86}Kr projectile with the neutron-rich ^{124,112}Sn targets at 25 MeV/nucleon where we used the ALADIN parametrization of high-energy fragmentation at 600 MeV/nucleon with the same ensemble approach in the present calculations. This shows the universality of the limitation of the excitation energy induced in the ensemble of projectile residues formed at low- and high-energy peripheral heavy-ion collisions. Our results demonstrate that neutron-rich systems produce the most neutron-rich isotopes. In addition to this work and studies in Refs. [6, 7], the same reactions have also been experimentally studied at 35 MeV/nucleon projectile energies by FAZIA group [12], and it was shown that the neutron-to-proton ratio of the final fragments clearly depends on the neutron richness of the target as a direct evidence of nucleon exchange between projectile and target. The findings of the theoretical interpretations of FAZIA experiments within SMM were also consistent with the experimental data [23]. In conclusion, our results may be used as a reference in the production of neutron-rich and neutron-poor rare isotopes in the chart of the nuclides toward the neutron and proton driplines. Extracted information from the analyses of this kind of experiments will play a key role in the knowledge of properties of exotic nuclei and for the simulation of the nuclear compositions in supernova explosion and the crust of neutron stars [24, 25]. Therefore, new experiments are needed for the future studies.

References

1. A. Kelić, K.-H. Schmidt, T. Enqvist et al., Isotopic and velocity distributions of Bi83 produced in charge-pickup reactions of Pb82208 at 1A GeV. Phys. Rev. C **70**, 064608 (2004). doi:10.1103/PhysRevC.70.064608
2. M. Bernas, C. Engelmann, P. Armbruster et al., Discovery and cross-section measurement of 58 new fission products in projectile-fission of 750 A MeV ^{238}U. Phys. Lett. B **415**, 111–116 (1997). doi:10.1016/S0370-2693(97)01216-1
3. H. Geissel, P. Armbruster, K.H. Behr et al., The GSI projectile fragment separator (FRS): a versatile magnetic system for relativistic heavy ions. Nucl. Instr. Meth. B **70**, 286–297 (1992). doi:10.1016/0168-583X(92)95944-M
4. H.M. Devaraja, S. Heinz, O. Beliuskina et al., Observation of new neutron-deficient isotopes with $Z \geq 92$ in multinucleon transfer reactions. Phys. Lett. B **748**, 199–203 (2015). doi:10.1016/j.physletb.2015.07.006
5. O. Beliuskina, S. Heinz, V. Zagrebaev et al., On the synthesis of neutron-rich isotopes along the N = 126 shell in multinucleon transfer reactions. Eur. Phys. J. A **50**, 161 (2014). doi:10.1140/epja/i2014-14161-3
6. P.N. Fountas, G.A. Souliotis, M. Veselsky et al., Systematic study of neutron-rich rare isotope production in peripheral heavy-ion collisions below the Fermi energy. Phys. Rev. C **90**, 064613 (2014). doi:10.1103/PhysRevC.90.064613
7. G.A. Souliotis, M. Veselsky, G. Chubarian et al., Enhanced production of neutron-rich rare isotopes in peripheral collisions at fermi energies. Phys. Rev. Lett. **91**, 022701 (2003). doi:10.1103/PhysRevLett.91.022701
8. A. Adare, S. Afanasiev, C. Aidala et al., Detailed measurement of the $e^+ + e^-$ pair continuum in $p + p$ and $Au + Au$ collisions at $sNN = 200$ GeV and implications for direct photon production. Phys. Rev. C **81**, 034911 (2010). doi:10.1103/PhysRevC.81.034911
9. D.V. Shetty, S.J. Yennello, G.A. Souliotis, Density dependence of the symmetry energy and the nuclear equation of state: a dynamical and statistical model perspective. Phys. Rev. C **76**, 024606 (2007). doi:10.1103/PhysRevC.76.024606
10. G.A. Souliotis, M. Veselsky, G. Chubarian et al., Enhanced production of neutron-rich rare isotopes in the reaction of 25 MeV/nucleon Kr-86 on Ni-64. Phys. Lett. B **543**, 163–172 (2002). doi:10.1016/S0370-2693(02)02459-0
11. Y.X. Zhang, C.S. Zhou, J.X. Chen et al., Correlation between the fragmentation modes and light charged particles emission in heavy ion collisions. Sci. China-Phys. Mech. Astron. **58**, 112002 (2015). doi:10.1007/s11433-015-5723-2
12. S. Barlini, S. Piantelli, G. Casini et al., Isospin transport in ^{84} Kr $+^{112,124}$ Sn collisions at Fermi energies. Phys. Rev. C **87**, 054607 (2013). doi:10.1103/PhysRevC.87.054607
13. Y.G. Ma, Application of information theory in nuclear liquid gas phase transition. Phys. Rev. Lett. **83**, 3617–3620 (1999). doi:10.1103/PhysRevLett.83.3617
14. A.S. Botvina, I.N. Mishustin, Statistical evolution of isotope composition of nuclear fragments. Phys. Rev. C **63**, 061601(R) (2001). doi:10.1103/PhysRevC.63.061601
15. J.P. Bondorf, A.S. Botvina, A.S. Iljinov et al., Statistical multifragmentation of nuclei. Phys. Rep. **257**, 133–221 (1995). doi:10.1016/0370-1573(94)00097-M
16. H. Imal, A. Ergun, N. Buyukcizmeci et al., Theoretical study of projectile fragmentation in the reactions ^{112} Sn $+^{112}$ Sn and ^{124} Sn $+^{124}$ Sn at 1 GeV/nucleon. Phys. Rev. C **91**, 034605 (2015). doi:10.1103/PhysRevC.91.034605
17. R. Ogul, A.S. Botvina, U. Atav et al., Isospin-dependent multifragmentation of relativistic projectiles. Phys. Rev. C **83**, 024608 (2011). doi:10.1103/PhysRevC.83.024608
18. R. Ogul, U. Atav, F. Bulut et al., Surface and symmetry energies in isoscaling for multifragmentation reactions. J. Phys. G: Nucl. Part. Phys. **36**, 115106 (2009). doi:10.1088/0954-3899/36/11/115106

19. N. Buyukcizmeci, H. Imal, R. Ogul et al., Isotopic yields and symmetry energy in nuclear multifragmentation reactions. J. Phys. G: Nucl. Part. Phys. **39**, 115102 (2012). doi:10.1088/0954-3899/39/11/115102
20. A. Ergun, H. Imal, N. Buyukcizmeci et al., Influence of angular momentum and Coulomb interaction of colliding nuclei on their multifragmentation. Phys. Rev. C **92**, 014610 (2015). doi:10.1103/PhysRevC.92.014610
21. A.S. Botvina, A.S. Iljinov, K.K. Gudima et al., Multifragmentation of highly excited nuclei in nucleus-nucleus collisions at intermediate-energies. Phys. At. Nucl. **57**, 628–635 (1994)
22. A.S. Botvina, I.N. Mishustin, M. Begemann-Blaich et al., Multifragmentation of spectators in relativistic heavy ion reactions. Nucl. Phys. A **584**, 737–756 (1995). doi:10.1016/0375-9474(94)00621-S
23. N. Buyukcizmeci, A. Ergun, H. Imal et al., Nucl. Sci. Tech. **26**, S20507 (2015). doi:10.13538/j.1001-8042/nst.26.S20507
24. A.S. Botvina, I.N. Mishustin, Statistical approach for supernova matter. Nucl. Phys. A **843**, 98–132 (2010). doi:10.1016/j.nuclphysa.2010.05.052
25. N. Buyukcizmeci, A.S. Botvina, I.N. Mishustin et al., A comparative study of statistical models for nuclear equation of state of stellar matter. Nucl. Phys. A **907**, 13–54 (2013). doi:10.1016/j.nuclphysa.2013.03.010